Chapter 1
Calibration of System Parameters Under Model Uncertainty

Ghina N. Absi and Sankaran Mahadevan

Abstract This paper investigates the quantification of errors and uncertainty in Bayesian calibration of structural dynamics computational models, affected by choices in model fidelity. Since Bayesian calibration uses an MCMC approach for sampling the updated distributions, using a high-fidelity model for calibration can be prohibitively expensive. On the other hand, use of a low-fidelity model could lead to significant error in calibration and prediction. This paper investigates model parameter calibration with a low-fidelity model corrected using higher fidelity simulations, and the trade-off between accuracy and computational effort. Different fidelity models may have different mesh resolutions, physics assumptions, boundary conditions, etc. The application problem used is of a curved panel located in the vicinity of a hypersonic aircraft engine, subjected to acoustic, thermal and aerodynamic loads. Two models are used to calibrate the damping characteristics of the panel: frequency response analysis and full time history analysis, and the trade-off between accuracy and computational effort is examined.

Keywords Multi-fidelity • Bayesian calibration • Hypersonic vehicle • Model uncertainty • Surrogate model

1.1 Introduction

Finite element analysis (FEA) is commonly used in the dynamic simulation of engineering structures with complicated geometry and under complex loading conditions. However, construction of the FEA model is subjective, affected by the engineer's assumptions. High-fidelity dynamic finite element analysis of complex systems is quite expensive, and considerable research has been done to construct cheaper and simpler surrogate models, equivalent static models, or reduced-order models. However, the errors and uncertainties increase with the reduction in model fidelity.

Two principal qualities are desired in a functional finite element model [1]: (1) physical significance: the model should correctly represent how the mass, stiffness and damping are distributed, and (2) correctness, where the response from dynamics experiments is accurately predicted by the model. Mottershead and Friswell [2] group modeling errors into three types: (a) model form errors (due to assumptions regarding the underlying physics of the problem, especially with strongly nonlinear behavior), (b) model parameter uncertainty (due to assumptions regarding boundary conditions, parameters distributions and simplifying assumptions), and (c) model order errors (arising from the discretization of complex geometry and loading). Computationally efficient models have to be cheap enough to allow multiple repetitions of the simulations, but also retain precious information available from rigorous more expensive models.

Many studies have concentrated on developing reduced-order models (ROM) to replace full fidelity dynamic analyses. McEwan [3, 4] proposed the Implicit Condensation (IC) method that included the non-linear terms of the equation of motion, but restricted the nonlinear function to cubic stiffness terms, and can only predict the displacements covered by the bending modes. Other methods explicitly include additional equations to calculate the membrane displacements in the ROM, such as those by Rizzi et al. [5, 6] and Mignolet et al. [7, 8].

Another direction of research to deal with inaccurate FEA is model updating. Direct updating methods have been proposed by computing closed-form solutions for the global stiffness and mass matrices using the structural equations of motion

G.N. Absi • S. Mahadevan (✉)
Department of Civil and Environmental Engineering, Vanderbilt University, Nashville, TN, USA
e-mail: sankaran.mahadevan@vanderbilt.edu

H.S. Atamturktur et al. (eds.), *Model Validation and Uncertainty Quantification, Volume 3: Proceedings of the 32nd IMAC, A Conference and Exposition on Structural Dynamics, 2014*, Conference Proceedings of the Society for Experimental Mechanics Series, DOI 10.1007/978-3-319-04552-8_1,

[9, 10]. The generated matrices are faithful to modal analyses, but do not always maintain structural connectivity, and may not always retain physical significance. Iterative methods study the changes in model parameterization to evaluate the type and the location of the erroneous parameters. and try to minimize the difference between the experimental data and the FE model predictions by varying these parameters [11]. In these cases, the mathematical model used in the model updating can sometimes be ill conditioned.

Liang and Mahadevan [12] replaced the expensive computational model with a surrogate model using Polynomial Chaos Expansion (PCE), and developed a systematic error quantification methodology. This approach facilitates running inexpensive simulations, while taking into account the resulting errors and uncertainties.

This paper considers Bayesian calibration of model parameters with experimental data, using a corrected low-fidelity model. It uses the information available in high-fidelity simulation to adjust the low-fidelity model, for better agreement with experimental results. The aim is to reduce the uncertainty in the parameters ahead of the final calibration (especially when a small number of experimental data is available), thus providing a stronger prior that takes into account additional high-fidelity information that may be missing in the low-fidelity model (such as non-linearity, additional variables, etc.). In the same way, information available in the low-fidelity model and missing from the high-fidelity one is retained, such as modeling the full domain (i.e. the full time history vs. a small segment). The corrected low-fidelity model is inexpensive, and becomes more accurate. This is particularly useful when limited experimental data are available, and the need of a reliable, yet fast model is essential.

1.2 Multi-fidelity Calibration Method

In this section, the concept of calibration is extended from a simple calibration using experimental data with a single model, to a sequential one, combining models of different fidelities. Assume that we have two models $G_1(X)$ and $G_2(X)$ of different fidelities. In order to achieve computational efficiency in Bayesian calibration, each model is replaced by fast running surrogate models $S_1(X)$ and $S_2(X)$. In order to build these surrogate models, the original models need to be evaluated multiple times. Assuming higher fidelity models run much slower than lower fidelity ones, time constraints will only allow fewer higher fidelity simulations.

1.2.1 Surrogate Model: Polynomial Chaos Expansion

Many surrogate modeling techniques have been developed in the literature, such as linear/quadratic polynomial-based response-surface [13], artificial neural networks [14], support vector machine (SVM) [15], polynomial chaos expansion (PCE) [16], and Gaussian process (GP) interpolation (or Kriging) [17]. In this paper, a PCE is used to replace the original models for inexpensive sampling in the calibration process. PCE is a regression-based surrogate model that represents the output of a model with a series expansion in terms of standard random variables (SRVs). Consider a model $y = f(\boldsymbol{x})$ where $\boldsymbol{x} = \{x_1, x_2, \ldots, x_k\}^T$ is a vector of input random variables. We construct a PCE to replace $f(\boldsymbol{x})$ using n multi-dimensional Hermite polynomials as basis functions:

$$y = \sum_{j=0}^{n} \theta_j \phi_j(\xi) = \theta^T \varphi(\xi) + \varepsilon_{surr} \tag{1.1}$$

where $\boldsymbol{\xi}$ is a vector of independent standard normal random variables which correspond to the original input x [18]. $\varphi(.) = \{\phi_0(.), \phi_1(.), \ldots, \phi_n(.)\}^T$ are the Hermite polynomial basis functions, and $\boldsymbol{\theta} = \{\theta_0, \theta_1, \ldots, \theta_n,\}^T$ are the corresponding coefficients that can be estimated by the least squares method. A collocation point method can be used to efficiently select training points where the original model is evaluated [19]. Suppose that m training points (ξ_i, y_i), $i = 1, 2, \ldots, m$ are available. Under the Gauss-Markov assumption [20], the surrogate model error ε_{surr} asymptotically follows a normal distribution with zero mean and variance given by

$$Var[\varepsilon_{surr}] \approx s^2 + s^2 \varphi(\xi)^T \left(\Phi^T \Phi\right)^{-1} \varphi(\xi) \tag{1.2}$$

where $\Phi = \{\varphi(\xi_1), \varphi(\xi_2), \ldots, \varphi(\xi_m)\}^T$ and $s^2 = \frac{1}{m-n} \sum_{i=1}^{m} \left[y_i - \theta^T \varphi(\xi_i)\right]^2$.

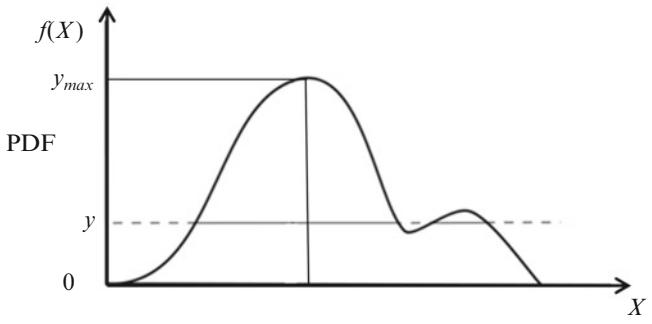

Fig. 1.1 Simple implementation of slice sampling

1.2.2 Uncertainty Quantification

The experimental output Y_{obs} is expressed in terms of the experimental input X, the errors and the model output as follows:

$$Y_{obs} + \varepsilon_{obs} = G\left(X + \varepsilon_{in}, \theta\right) + \varepsilon_{surr} + \varepsilon_{mf} \tag{1.3}$$

where

ε_{in}: input experimental error
ε_{mf}: model form error (calculated automatically within the code)
ε_{surr}: surrogate model error
ε_{obs}: output experimental error

In order to get accurate calibration results, these errors need to be included in the calibration [21]. The experimental measurement errors ε_{in} and ε_{obs} are represented as random variables, with known (or assumed) distributions. The surrogate model error ε_{surr} reflects the uncertainty we have regarding the replacement of the original model with a response surface model, as is shown in Eq. 1.2. As for the model form error ε_{mf}, it is calibrated along with model parameters using experimental data, following Eq. 1.3.

1.2.3 Bayesian Calibration

Three approaches are available for calibration: least squares, maximum likelihood, and Bayesian calibration. This paper uses Bayesian calibration since it is the most comprehensive approach, allowing uncertainty quantification of the calibration result.

The Bayesian calibration is based on Bayes' theorem:

$$f_{\mathrm{X}}(x|\,\mathrm{D}) \propto f_{\mathrm{X}}(x).L(x) \tag{1.4}$$

where $f_{\mathrm{X}}(x \mid \mathrm{D})$ is the posterior distribution of the variable X after calibration using the data D, $f_{\mathrm{X}}(x)$ is the prior distribution of X (assumed by the user), and $L(x)$ is the likelihood function (probability of observing the data D, given a calibration parameter value). Sampling from the posterior is done using a Markov Chain Monte Carlo (MCMC) algorithm. Several algorithms are available for MCMC sampling: Metropolis-Hastings [22], Gibbs sampling [23], slice sampling [24], etc. Slice sampling is used in the numerical example to evaluate Eq. 1.4. It is based on the observation that to sample a random variable, one can sample uniformly from the region under the PDF. The simplest implementation (for a uni-variate distribution without the need to reject any points) consists of first sampling a random value y between 0 and the maximum PDF value y_{max}. The next step is to sample x from the slice under the PDF, as shown in Fig. 1.1.

Slice sampling requires many simulations of the model used. Low-fidelity models are fast, but inaccurate. High-fidelity models are more reliable, but time-consuming. Therefore we propose correcting the low-fidelity model first with high-fidelity simulations, and using the corrected model for calibration with experimental data.

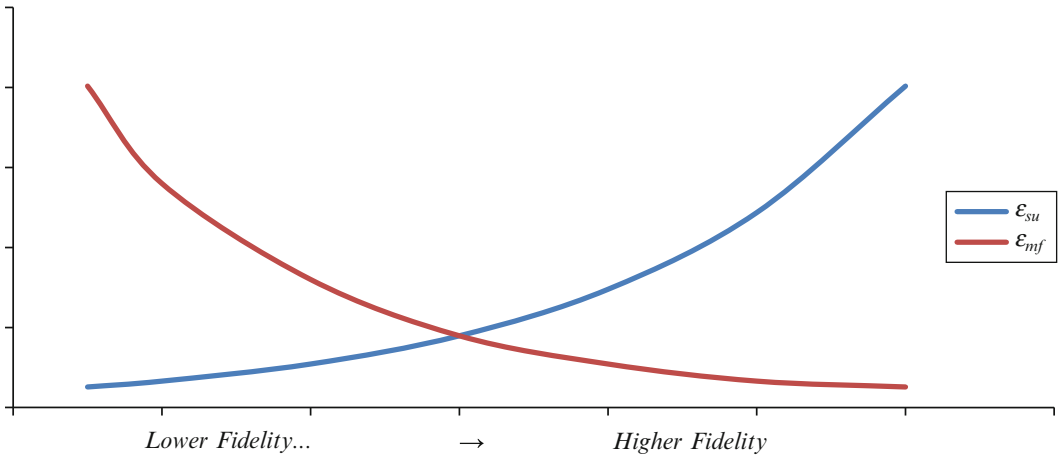

Fig. 1.2 Variation of ε_{sur} and ε_{mf} with model fidelity

1.2.4 Validation

Model validation is used to determine the degree of agreement of a model prediction with observed experimental data, and compare multiple models to determine which one is better supported by the data. Many methods have been proposed that include parametric uncertainty [25]. For two models (denoted by M_i and M_j) with prior probabilities of acceptance P(M_i) and P(M_j), the relative posterior probabilities can be computed using Bayes' rule [26, 27]:

$$\frac{P\left(M_i \middle| Observation\right)}{P\left(M_j \middle| Observation\right)} = \frac{P\left(Observation \middle| M_i\right)}{P\left(Observation \middle| M_j\right)} \frac{P\left(M_i\right)}{P\left(M_j\right)} \tag{1.5}$$

The likelihood ratio $\frac{P\left(Observation \middle| M_i\right)}{P\left(Observation \middle| M_j\right)}$ is referred to as "Bayes factor", and is used as the metric to assess the data support to Model M_i relative to model M_j. If the Bayes factor is greater than 1.0, then it can be concluded that the model M_i is more supported by the data.

1.2.5 Multi-fidelity Implementation

Let N_1 and N_2 denote the number of simulations available for each original model G_1 and G_2, uniformly distributed over the problem domain. These realizations are used to build the corresponding surrogate models. Because of time and budget constraints, we assume that higher the fidelity of the model, the lower the number of simulations available, i.e.: $N_2 \leq . N_1$. This results in a surrogate model error for G_2 larger than that for G_1. However, since G_2 is of a higher fidelity than G_1, the model form error in G_1 is larger than that for G_2, i.e., $\varepsilon_{mf(1)} \geq \varepsilon_{mf(2)}$. Figure 1.2 shows a notional diagram of how the surrogate model error and model form error might vary with the fidelity of the model.

The proposed approach avoids the need to build a surrogate model for the high-fidelity simulations, and thus avoids the high surrogate model error that comes with it. It uses the available simulations of the high-fidelity model to correct the low-fidelity surrogate model, and uses the latter in the calibration process.

The multi-fidelity calibration algorithm is as follows:

(i) *Run the Low (G_1) and High (G_2) fidelity models to obtain N_1 and N_2 sets of outputs, respectively.*
(ii) *Build S_1, the surrogate model replacing G_1. In this step, the variance of S_1 is calculated to account for the surrogate model error.*
(iii) *Define the priors of the calibration parameters, and the discrepency between the models $D_{2,1}$.*
(iv) *Calibrate the parameters of low-fidelity model as well as the discrepency with the high-fidelity simulations.*

(v) *Set the corrected low-fidelity model as*: $LF_{corr} = LF + D'_{2,1}$, *where* $D'_{2,1}$ *is the posterior of* $D_{2,1}$ *obtained from step iv.*
(vi) *Assume a prior distribution for the model form error* ε_{mf}.
(vii) *Re-calibrate the dynamics model parameters along with* ε_{mf} *with the available experimental data. Use the posteriors of the dynamics model parameters from step iv. as priors* ($D'_{2,1}$ *is fixed in this step based on the result in step v*).

This approach allows the use of the information from both fidelity models, with minimal surrogate model error.

1.3 Numerical Example

1.3.1 Problem Description

The application problem is of a hypersonic airplane fuselage panel located next to the engine, subjected to dynamic acoustic loading (AL). The panel is curved, as shown in Fig. 1.3, and is modeled using the FEA software ANSYS. The strain at seven different locations of the panel is recorded.

The damping—to be calibrated—is modeled as frictional damping for a width of "1" around the perimeter of the panel, and material damping for the rest of the panel area. The boundary fixity is also a calibration variable, and is described by a fixity ratio FR = length of plate perimeter fixed/total boundary length (see Fig. 1.4).

Two models of different fidelities were considered:

– Model 1: A power spectral density analysis, which consists of a linear combination of mode shape effects
– Model 2: A full transient analysis where the acoustic loading is applied as a dynamic time history input.

Model 1 and Model 2 have the finite element mesh, and the materials, the boundary conditions and the mesh resolution are the same. They differ in the application of loads, the analysis method, and the output type.

In Model 1, the input acoustic load applied is the Welch power spectral density (PSD) [28] of the experimental 140 dB acoustic load. The PSD describes how the power of a signal or time series is distributed over the different frequencies. For a signal $X(t)$, it is calculated as follows:

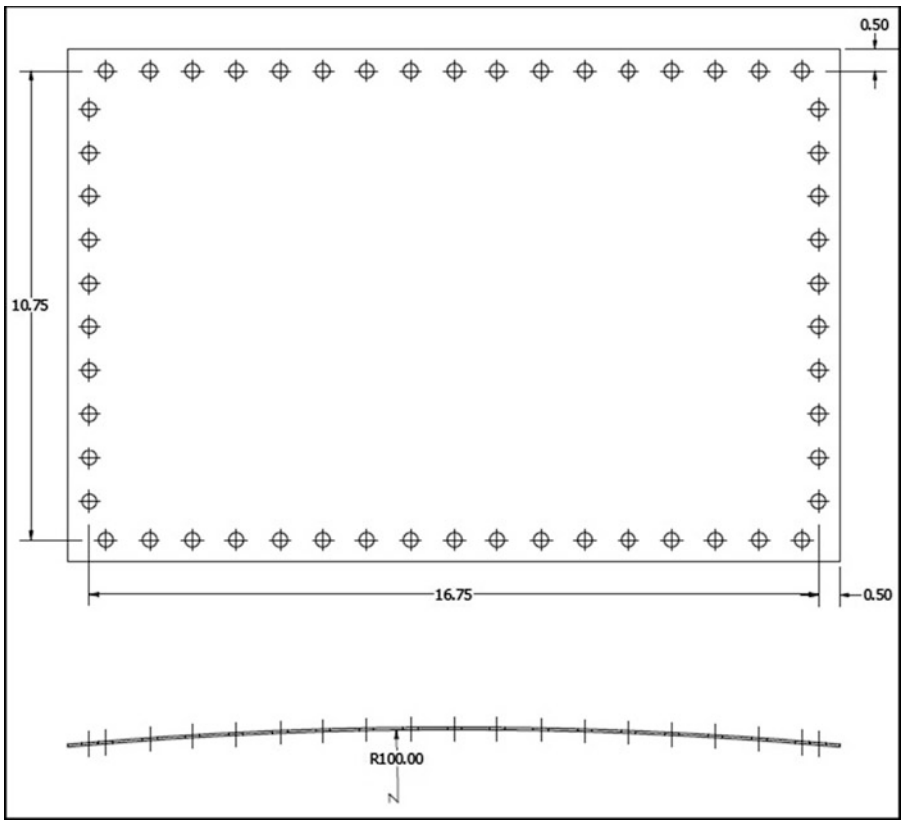

Fig. 1.3 Curved panel dimensions

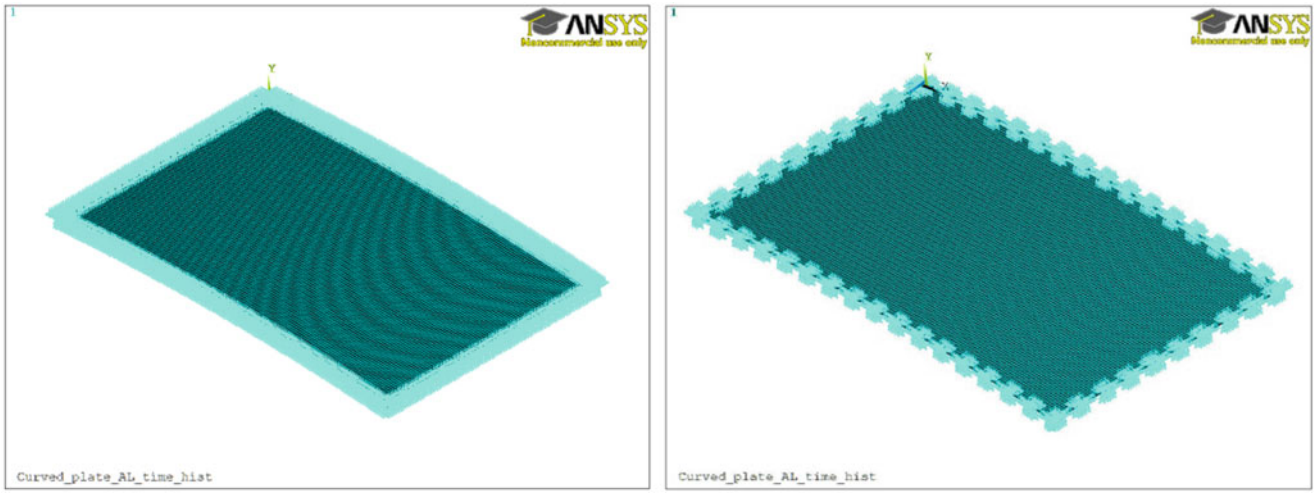

Fig. 1.4 Example of FR = 1 and 0.5

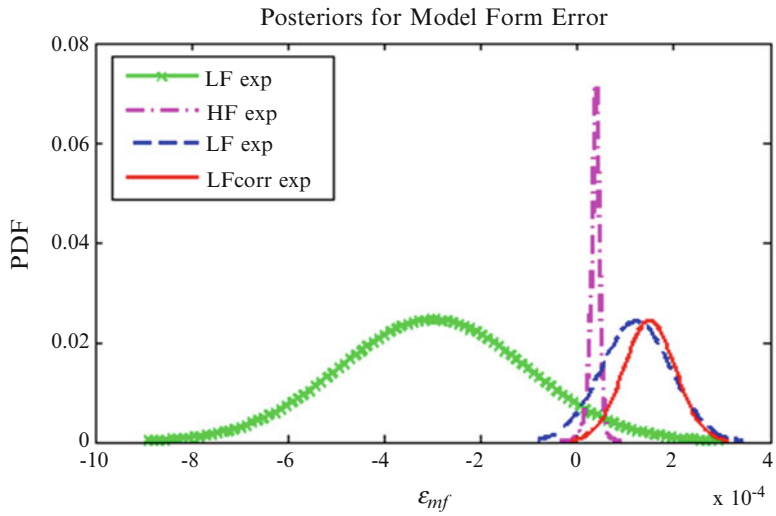

Fig. 1.5 Model form errors posteriors

$$S_{xx}(\omega) = \lim_{T\to\infty}\left[\frac{E\left[|F_{X_T}(\omega)|^2\right]}{2T}\right] \tag{1.6}$$

where $E[]$ is the expected value, and $F_{X_T}(\omega) = \int_{-\infty}^{\infty} X_T(t)e^{-jwt}dt$ the Fourier transform of $X(t)$.

The PSD is calculated with the entire 140 dB signal, for the full duration of 60 s. However, it is not unique to the signal it is calculated from, because the phase component is discarded. For different phase relationships, different time-domain signals fit the same PSD. Also, the spectrum analysis in ANSYS is a linear combination of the mode effects on the structure. Finally, even though Model 1 is inexpensive to run (one simulation takes about 9.5 min to complete), it does not allow the user to add initial conditions on the structure such as initial stress resulting from fixing the plate on the test-rig (a uniform load has a PSD of 0, and will not contribute to the RMS strain output).

Model 2, in contrast, is a full transient dynamic analysis of the panel. The model run is quite time-consuming, allowing only 0.2 s of the input signal (of the full 60 s of data available) to be simulated, and each simulation takes 5.5 h (35 times slower than Model 1). However, Model 2 does allow us the addition of initial stress on the model, and preliminary test runs have shown that a uniform initial load on the panel is consistent with the experimental observation (see Fig. 1.5).

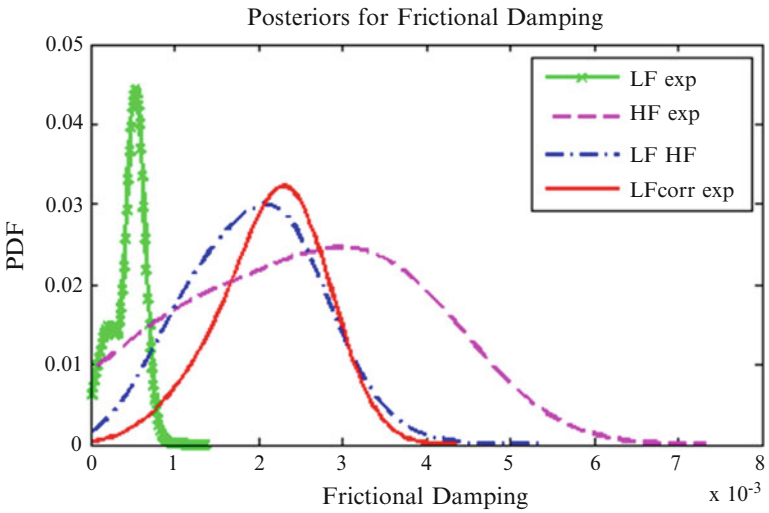

Fig. 1.6 Frictional damping posteriors

The hypothesis of this paper is that initial correction of the low-fidelity model with the higher fidelity model allows us to use information from both in the final calibration of the system parameters, i.e., the full length of the signal in the form of the PSD, and the transient behavior as well as the initial conditions incorporated in the full dynamic analysis.

1.3.2 Results

Four calibration results are being compared in this section: The low-fidelity model calibrated with experimental data (LF_exp), the high-fidelity model calibrated with experimental data (HF_exp), the low-fidelity model calibrated with the high-fidelity simulations (LF_HF) and the corrected low-fidelity model calibrated with the experiments data (LFcorr_exp).

The following priors are assumed for the calibration parameters:

$\varepsilon_{mf} \sim$U $[-10^{-1}, 10^{-1}]$
FR_DC$\sim$U $[10^{-4}, 10^{-2}]$—Frictional damping coefficient
MT_DC$\sim$U $[5.10^{-7}, 10^{-4}]$—Material damping coefficient
FR$\sim$U [0.7, 1]—Fixity ratio

$\varepsilon_{obs} \sim$N $(0, \sigma_{obs})$ where the prior of σ_{obs} follows a Jeffreys distribution [29] with bounds $[10^{-5}; 10^{-2}]$: with a fixed $\mu_{obs} = 0$, the prior of σ_{obs} is assumed as $\pi(\sigma) \propto 1/\sigma$. The low-fidelity model was run 40 times, whereas the high-fidelity was run nine times. We only have one set of experimental data available (one observation at each strain gage location). Four strain gage outputs are used for calibration, and a fifth is used to compute the Bayes factor (likelihood ratio) to compare the results of the different calibration options. The following figures show the posteriors of the model form errors (Fig. 1.5), frictional (Fig. 1.6) and material (Fig. 1.7) damping and the fixity ratio (Fig. 1.8).

Using the fifth (validation) data set, the likelihood ratios among the three calibration options were computed as

$$\text{LF} : \text{LFcorr} : \text{HF} = 1 : 1.31 : 1.29$$

1.3.3 Discussion

The main difference between Models 1 and 2, besides the analysis type, is the initial stress added in Model 2, in the form of a distributed uniform load. Preliminary testing of Model 2 with and without initial stress showed that, without adding a uniform load on the panel, the strain amplitude was much lower than the experimental output, as seen in Fig. 1.9.

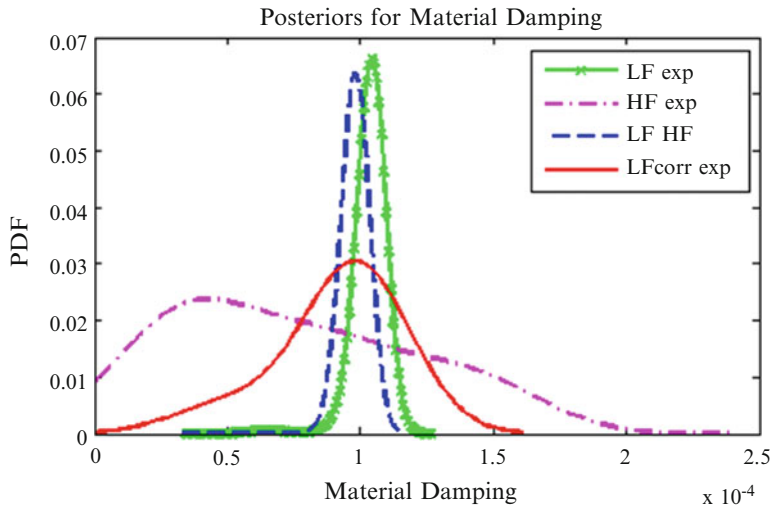

Fig. 1.7 Material damping posteriors

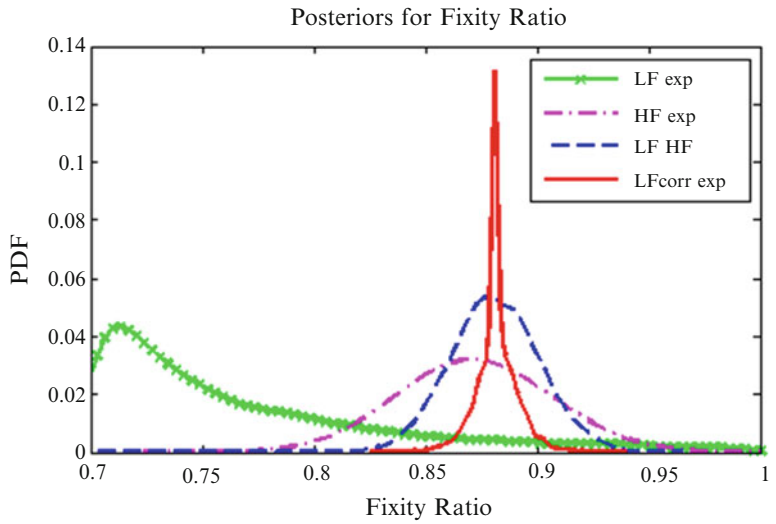

Fig. 1.8 Fixity ratio posteriors

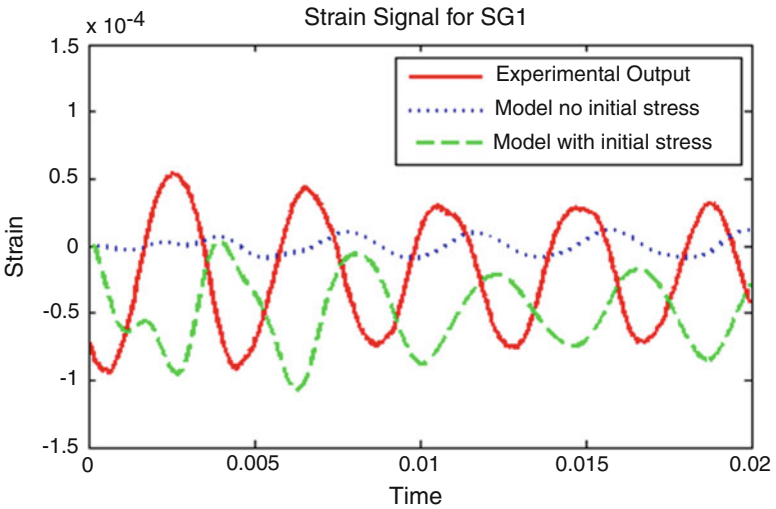

Fig. 1.9 Preliminary model testing

The calibration results show the effect of ignoring the initial stress. The posteriors from the calibration with Model 1 (the low-fidelity model) underestimate the damping and the fixity ratio, in an attempt to recover the energy under the PSD curve (strain RMS) which is directly proportional to the signal amplitude. This loss of accuracy is also shown in the model form error, which is much greater (in magnitude) than the rest of the models.

Not only were the results in favor of the use of the corrected low-fidelity model in the calibration process, but its convergence was faster than both low-fidelity and high-fidelity calibrations with experimental data. Slice sampling was required to give 8,000 accepted samples of the parameters posterior distributions. The corrected low-fidelity model needed 25,284 samples to accept 8,000, whereas using the high-fidelity model alone for calibration needed 40,352 samples, and using the low-fidelity model alone needed 95,327 samples.

Furthermore, the likelihood ratio calculated in Sect. 1.3.2 shows that the calibration result of the corrected low-fidelity model is almost as acceptable as the high-fidelity model. When this likelihood comparison is considered along with the computational efficiency of the two-step approach, it appears that the proposed methodology offers a reasonable trade-off between accuracy and computational effort.

1.4 Conclusion

This paper investigated the use of multi-fidelity models in the calibration of model parameters. Time-consuming high-fidelity simulations were used to correct the inexpensive low-fidelity model, and the corrected low-fidelity model was used for parameter calibration with experimental data. This efficient two-step method allows the fusion of information from both model fidelities, and is particularly useful when only a small number of experimental data points is available.

Future work needs to investigate the efficacy of this approach when more than two models are available, and find a systematic quantitative way of using the available information. The calibration becomes more complicated when the damping is load-dependent, and future work needs to account for this dependence. The extension to multiple physics with the application of thermal and aerodynamic loads also needs to be studied in the future.

Acknowledgement The research reported in this paper was supported by funds from the Air Force Office of Scientific Research (Project Manager: Dr. Fariba Fahroo) through subcontract to Vextec Corporation (Investigators: Dr. Robert Tryon, Dr. Animesh Dey). The support is gratefully acknowledged. The computations in the numerical example were partly conducted using the resources at the Advanced Computing Center for Research and Education (ACCRE) at Vanderbilt University.

References

1. Caesar B (1987) Updating system matrices using modal test data. In: Proceedings of the fifth IMAC, pp 453–459
2. Mottershead JE, Friswell MI (1993) Model updating in structural dynamics: a survey. J Sound Vib 167:347–375
3. McEwan M, Wright JR, Cooper JE, Leung YT (2001) A finite element/modal technique for nonlinear plate and stiffened panel response prediction, AIAA-2001-1595
4. McEwan M (2001) A combined modal/finite element technique for the non-linear dynamic simulation of aerospace structures. PhD. dissertation, University of Manchester, England
5. Muravyov A, Rizzi S (2003) Determination of nonlinear stiffness with application to random vibration of geometrically nonlinear structures. Comput Struct 81:1513–1523
6. Rizzi S, Przekop A (2008) System identification-guided basis selection for reduced-order nonlinear response analysis. J Sound Vib 315:467–485
7. Mignolet M, Radu A (2003) Validation of reduced order modeling for the prediction of the response and fatigue life of panels subjected to thermo-acoustic effects, Structural dynamics: recent advances. In: Proceedings of the eighth international conference, University of Southampton, England
8. Kim K, Wang XQ, Mignolet MP (2003) Nonlinear reduced order modeling of functionally graded plates, AIAA-2008-1873
9. Baruch M, Bar-Itzhack IY (1978) Optimal weighted orthogonalization of measured modes. AIAA J 16:346–351
10. Berman A, Nagy EJ (1983) Improvement of large analytical model using test data. AIAA J 21:1168–1173
11. Link M (1999) Updating of analytical models—review of numerical procedures and application aspects. Structural dynamics forum SD2000, Los Alamos
12. Liang B, Mahadevan S (2011) Error and uncertainty quantification and sensitivity analysis in mechanics computational models. Int J Uncertain Quantif 1(2):147–161
13. Faravelli L (1989) Response-surface approach for reliability analysis. J Eng Mech 115(12):2763–2781
14. Hurtado JE, Alvarez D (2001) Neural-network-based reliability analysis: a comparative study. Comp Methods Appl Mech Eng 191(1–2): 113–132
15. Rocco C, Moreno J (2002) Fast Monte Carlo reliability evaluation using support vector machine. Reliab Eng Syst Saf 76(3):237–243

16. Ghanem RG, Spanos P (1991) Stochastic finite elements: a spectral approach. Springer, Berlin
17. Romero V, Swiler L, Giunta A (2004) Construction of response surfaces based on progressive-lattice-sampling experimental designs with application to uncertainty propagation. Struct Saf 26(2):201–219
18. Isukapalli SS (1999) Uncertainty analysis of transport-transformation. Ph.D. thesis, The State University of New Jersey, Rutgers
19. Huang SP, Mahadevan S, Rebba R (2007) Collocation-based stochastic finite element analysis for random field problems. Probab Eng Mech 22(2):194–205
20. Seber GAF, Wild CJ (1989) Nonlinear regression. Wiley, New York
21. Kennedy MC, O'Hagan A (2001) Bayesian calibration of computer models. J R Stat Soc 63(3):425–464
22. Hastings W (1970) Monte Carlo sampling methods using Markov chains and their application. Biometrika 57(1):97–109
23. Casella G, George E (1992) Explaining the Gibbs sampler. Am Stat 46(3):167–174
24. Neal R (2003) Slice sampling. Ann Stat 31(3):705–741
25. Oberkampf WL, Trucano TG (2002) Verification and validation in computational fluid dynamics. Progr Aerosp Sci 38:209–272
26. Berger JO, Pericchi LR (1996) The intrinsic Bayes factor for model selection and prediction. J Am Stat Assoc 91:109–122
27. Leonard T, Hsu JSJ (1999) Bayesian methods: an analysis for statisticians and interdisciplinary researchers. Cambridge University Press, Cambridge
28. Welch PD (1967) The use of fast Fourier transform for the estimation of power spectra: a method based on time averaging over short, modified periodograms. IEEE Trans Audio Electroacoust AU-15:70–73
29. Kass RE, Wasserman L (1996) The selection of prior distributions by formal rules. J Am Stat Assoc 91(435):1343–1370